COMMUNICATION

Multiferroic Nanopatterned Hybrid Material with Room-Temperature Magnetic Switching of the Electric Polarization

*Ronggang Cai, Vlad-Andrei Antohe, Zhijun Hu, Bernard Nysten, Luc Piraux, and Alain M. Jonas**

The possibility to store and retrieve information using orthogonal write and readout channels offers sturdier storage and access to entirely new device configurations.[1] An especially important practical case is writing with a magnetic field an information stored as the direction of an electric dipole; unfortunately, magnetic fields do not act on static electric dipole moments. For some multiferroic materials in which the ferroelectric and magnetic orders are intrinsically coupled in the crystal unit cell, reversal of the electric polarization is possible upon application of a magnetic field;[2–4] however, this mostly happens at temperatures well below room temperature, or at room temperature in very few materials such as solid solution phases between lead zirconium titanate and lead iron tantalate[5] and in multiferroic Aurivillius phases.[6] Here, we design a nanopatterned hybrid layer wherein the electric polarization can be flipped at room temperature by a magnetic field aided by an electrical field. This is achieved by embedding ferromagnetic nanopillars in a continuous organic ferroelectric layer, and amplifying the magnetostriction-generated stress gradients by scaling down the supracrystalline cell of the material. The resulting layer offers magnetically tunable electrically encoded information in an inherently regularly nanopatterned medium.

Multiferroics are materials exhibiting the coexistence of different ferroic orders, such as ferromagnetism and ferroelectricity;[7–9] when these two orders are coupled, magnetoelectricity ensues. It can be intrinsic as in magnetic atom-containing perovskite compounds,[2–6,10] charge transfer complexes,[11–14] or magnetic metal-organic frameworks;[15,16] or result from the coupling of two ferroic orders located in different intimately mixed phases which interact mechanically, as in extrinsic magnetoelectric composite materials and devices.[17–19] In such composites made of a ferroelectric and a ferromagnetic material, the coupling of the two ferroic orders is mediated by strains arising from piezoelectricity and magnetostriction. In these materials, the electric polarization can be tuned by the application of an external magnetic field; however, the electric polarization could so far not be fully and permanently reversed by a magnetic field in such materials, which is required for memory applications.

Here, we design a regular multiferroic organic/inorganic layer of 1–3 connectivity,[20] in which ferromagnetic nickel (Ni) nanopillars are embedded in a nanostructured ferroelectric polymer matrix over centimeter scale surfaces. The ferroelectric continuous phase is poly(vinylidene fluoride-*ran*-trifluoroethylene) (P(VDF-TrFE));[21] it was selected for its high remnant polarization, short switching time, low processing temperature, and small Young's modulus, allowing it to be easily deformed by the much more rigid ferromagnetic pillars. Accordingly, PVDF-based multiferroic materials can exhibit very large magnetoelectric coefficients.[22] Ni was selected as the ferromagnetic component owing to its relatively large magnetostrictive coefficient $\lambda = \Delta L/L$, where L is the length of the sample ($\lambda = -3.5 \times 10^{-5}$ in bulk isotropic Ni).[23]

The multiferroic layer was made by a parallel process (**Figure 1**a and the Experimental Section) involving shaping a spincoated P(VDF-TrFE) film with a mold having cylindrical pillars of 65 nm diameter and 90 nm height arranged over a square lattice of 190 nm unit cell size, corresponding to a theoretical storage density of more than 10 Gbit in.$^{-2}$. After removing the mold, a ca. 80 nm thick P(VDF-TrFE) layer (Figure 1b,c) with holes of 65 nm diameter fully opened down to the bottom Ag electrode was obtained; the ferroelectric layer is semicrystalline with essentially random orientation as shown by grazing angle X-ray scattering (Figure S1, Supporting Information). Thereafter, Ni nanopillars of ca. 65 nm height were grown in the templating layer by pulsed electrochemical deposition (Figure 1d–f).

The macroscopic magnetic hysteresis loops of the sample measured with the magnetic field in the out-of-plane and in-plane directions indicate magnetic anisotropy with the easy axis lying in the sample plane (Figure S2, Supporting Information), due to the relatively flat circular pillars and dipolar coupling between neighboring pillars. The most probable magnetization configuration in the remanent state for low aspect-ratio Ni nanopillars is a closed vortex structure, consisting of circumferential in-plane magnetization with an out-of-plane component near the central position.[24]

Because the Ni nanopillars are electrically conducting, the ferroelectric properties of the polymer matrix were probed locally by piezoresponse force microscopy (PFM),[25,26] with the PFM tip acting as mobile electrode. Reversal of the polarization

Dr. R. Cai, Dr. V.-A. Antohe, Prof. B. Nysten, Prof. L. Piraux, Prof. A. M. Jonas
Institute of Condensed Matter and Nanosciences
Université catholique de Louvain
Croix du Sud 1/L7.04.02
1348 Louvain-la-Neuve, Belgium
E-mail: alain.jonas@uclouvain.be
Prof. Z. Hu
Center for Soft Condensed Matter Physics and Interdisciplinary Research
Soochow University
215006 Suzhou, China

DOI: 10.1002/adma.201604604

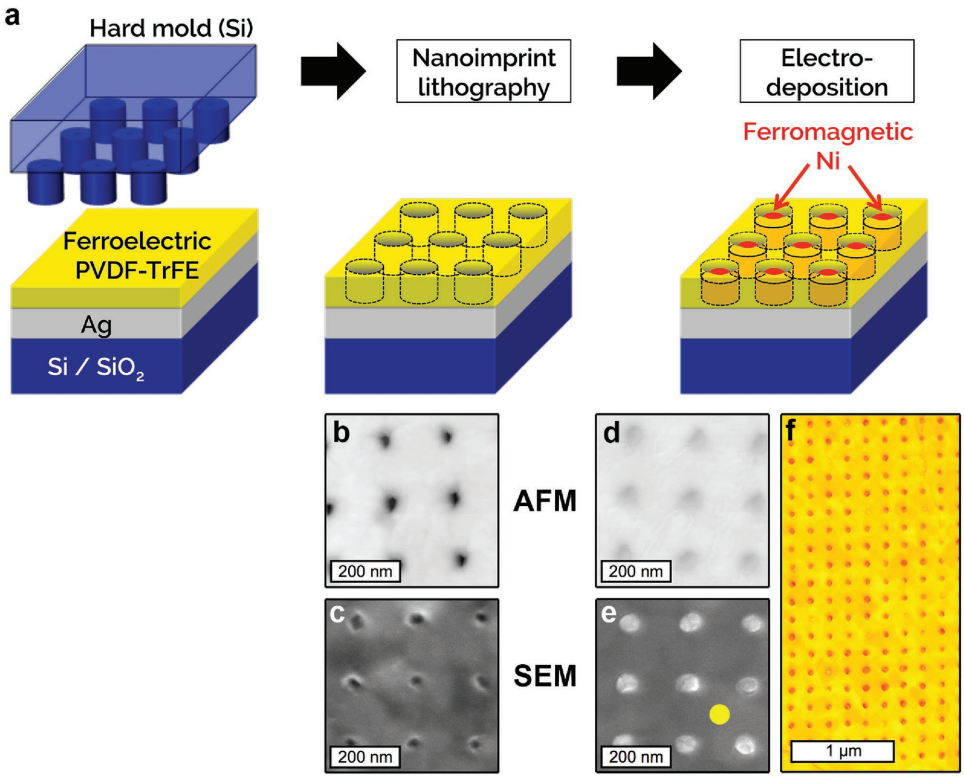

Figure 1. a) Fabrication process and morphology of the layer b,c) before and d–f) after electrodeposition of the ferromagnetic metal. AFM topography images (b, d) are displayed with the same gray scale from –80 nm (black) to 10 nm (white), to show the filling of the pores by Ni. The top surface of the Ni pillars is 10–15 nm below the average height of the polymer film. Panels (c, e, f) are SEM images, (f) being in false colors to emphasize composition; the yellow dot in (e) shows the typical location of the PFM tip when probing ferroelectric hysteresis loops.

of the P(VDF-TrFE) matrix upon electrical poling was verified by PFM images (Figure S3, Supporting Information). The tip was then placed at the center of a supracrystalline unit cell (yellow dot in Figure 1e), and vertical PFM hysteresis loops were recorded in the presence and absence of a vertical magnetic field. Finite element modeling (Comsol Multiphysics; Figure S4, Supporting Information) shows that the electric field concentrates in a small region of the polymer matrix just below the PFM tip.

The ease of switching of the electrical polarization (by the DC bias of ±10 V) was found to depend on magnetic field: indeed, the width of the hysteresis loops decreased dramatically with increasing magnetic field (**Figure 2**a,b); the effect was reproduced for another PFM measurement frequency (**Figure 3**a). Of note, the hysteresis loops are off-centered, which may be due to the difference of work function of the bottom and top electrodes, and/or the existence of other electrostatic couplings in the PFM equipment. Nevertheless, this shift does not change the qualitative evolution of the hysteresis, nor influences the analysis of the width of the hysteresis loops. The dependence of the ferroelectric hysteresis loop width (FHLW) on magnetic field strikingly parallels the variation of the magnetization of Ni versus vertical magnetic field (Figure 2b). Experiments performed with another magnet allowing us to reverse the direction of the magnetic field also show that the FHLW is an even function of the magnetic field, as is magnetostriction (Figure S5, Supporting Information).

A second, independently prepared sample exhibited the same behavior. Similar experiments were also performed on control samples. A patterned sample in which paramagnetic Pt replaces ferromagnetic Ni pillars, and a simple 80 nm thick P(VDF-TrFE) layer, do not exhibit a significant sensitivity to the magnetic field (Figure S6a,b, Supporting Information); nor does a bilayered multiferroic sample consisting of a continuous P(VDF-TrFE) layer over a thin continuous Ni layer (Figure 2b). In the latter case, the magnetostriction-induced dimensional changes of Ni are strongly reduced due to its clamping to the substrate, as supported by theoretical predictions[27] and experimental observations[17] on inorganic composite multiferroics. Finally, a sample prepared with a 2.5 times larger supracrystalline unit cell and a smaller Ni volume fraction exhibited a weaker effect, indicating the importance of dimensional parameters (Figure S6c, Supporting Information).

Since the magnetostriction coefficient is negative in Ni, an out-of-plane magnetic field leads to a contraction of the Ni nanopillars along the field direction and to an expansion of the pillars in the plane of the substrate. At the bottom of the pillars, the expansion is considerably reduced by clamping. However, near the top of the pillars, Ni expands in-plane, leading to compression and shear of the polymer matrix. Notably, the deformation might be enhanced because of the in-plane vortex configuration, especially considering that magnetostriction coefficients could be larger in nanoparticles than in bulk materials.[28] The mechanical energy stored in the semicrystalline polymer then

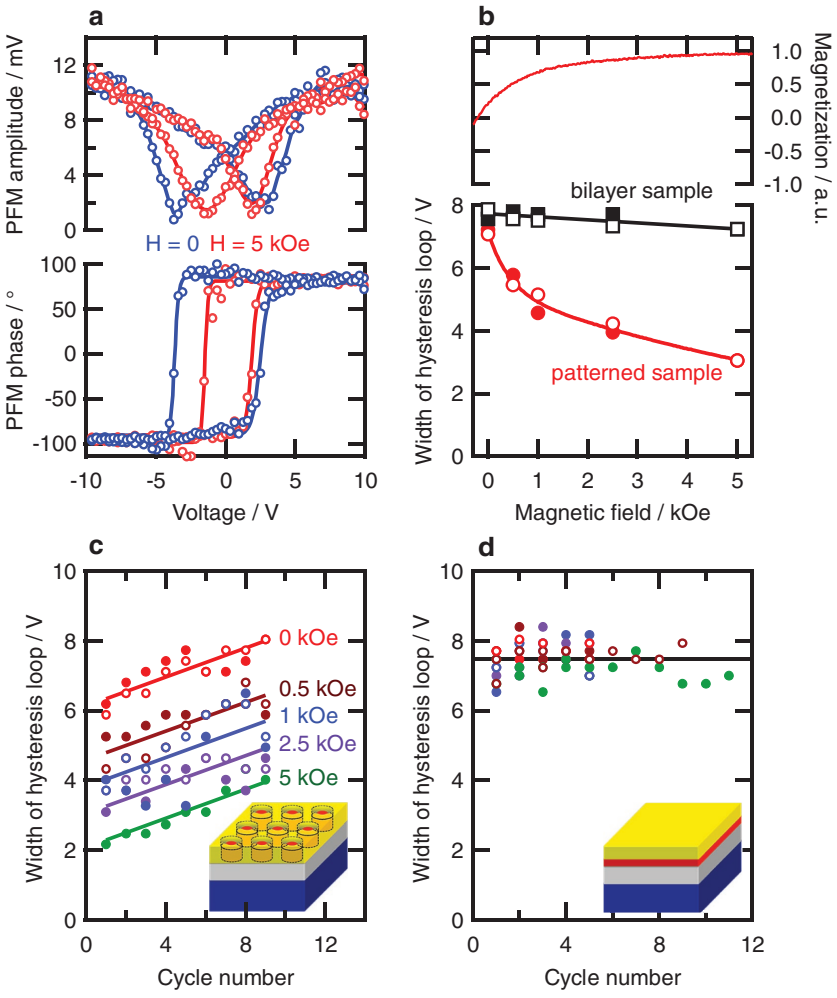

Figure 2. a,b) The application of a magnetic field decreases the width of the ferroelectric hysteresis loop of the patterned multiferroic layer, and c) repeated measurements of the ferroelectric hysteresis loop at a given value of magnetic field broaden the loop for the patterned sample, d) not for the bilayered sample. Panel (a) shows the ferroelectric hysteresis loops acquired for two values of the magnetic field, for the patterned sample. The bottom part of panel (b) compares the variation of the width of the ferroelectric hysteresis loop with the applied magnetic field, for the patterned sample and a bilayered Ni/P(VDF-TrFE) control (reference) sample. Solid symbols correspond to measurements performed while increasing the magnetic field; open symbols to the reverse. The top graph in panel (b) is the out-of-plane magnetization measured on the patterned sample, versus magnetic field. For the measurements displayed in panels (c, d), the field was increased after each series of measurements at a given value of magnetic field (solid symbols); then, after reaching 5 kOe, the field was decreased (open symbols). The same color code is used in panels (c) and (d). The PFM acquisition frequency was 15 kHz.

presumably contributes to lower the barriers to the motion of polymer segments, and therefore to decrease the coercive field and ease polarization switching, which involves rapid rotation of chain stems in crystals and slower segmental motion in amorphous regions.[29] A further possible contribution is from the flexoelectricity of ferroelectric materials, i.e., the coupling of electric polarization and strain gradients, an effect recently used to switch electric polarization by the local application of a stress.[30] Flexoelectricity is actually a possible reason for the observed off-centering of hysteresis loops. Flexoelectricity is especially large in PVDF-based copolymers,[31] and strain gradients are magnified by the small dimensions of the supracrystalline cell.[32]

The importance of internal stresses and strains is further supported by the observation that, when the ferroelectric hysteresis is repeatedly probed at a given value of magnetic field, the FHLW increases continuously for the patterned sample (Figure 2c), whereas it is constant for the bilayered reference sample (Figure 2d). This is because, in the patterned sample, the stresses in the ferroelectric polymer are progressively relaxed by the segmental motions resulting from repeated ferroelectric switching; therefore, switching becomes more difficult and the coercive electric field increases. Interestingly, the hybrid layer at zero magnetic field also exhibits progressive broadening of the loops upon successive cyclic probing, due to the initial mechanical stresses in the polymer following the growth of Ni pillars, that are also relaxed by segmental motions upon cyclic probing. The same logically holds true for the nonferromagnetic sample wherein Pt replaces Ni pillars, which also displays a FHLW depending on probing cycle but without significant dependence on magnetic field (Figure S7, Supporting Information).

An attempt was performed to reverse the polarization of the ferroelectric polymer by a magnetic field, keeping the voltage just below the switching voltage (V_1 in Figure 3a). The voltage was swept from –10 to 10 V, then back to –10 V to polarize the sample upward. Then, the voltage was set to V_1, which is too low to flip the polarization. When the magnetic field was subsequently switched from 0 to 5 kOe (Figure 3b), the PFM phase changed by ca. 140°, close to the 180° variation expected for the full reversal of the direction of polarization. However, the change was not permanent, and the electric polarization returned back to its original value upon removal of the magnetic field. Therefore, stress relaxation was used to broaden the polarization switching magnetic window: the starting state was prepared by first relaxing the stresses in the polymer by measuring cyclically ca. ten ferroelectric loops at zero applied magnetic field; then, the scans were stopped while keeping ca. 1.2 V on the PFM tip (V_2 in Figure 3a). When the magnetic field was subsequently switched to 5 kOe, the PFM phase dropped from ca. 80° to –70° with only a small variation of PFM amplitude (Figure 3c), indicating flipping of the electrical polarization from the almost stress-relaxed 0 Oe state to a stress-unrelaxed 5 kOe state. The switching of the polarization is now permanent and insensitive to subsequent variations of magnetic field, with only a small relaxation observed with time. When a similar switching test was performed on the bilayered P(VDF-TrFE)/Ni control sample (Figure 3d), the PFM phase and amplitude were logically essentially insensitive to the magnetic field.

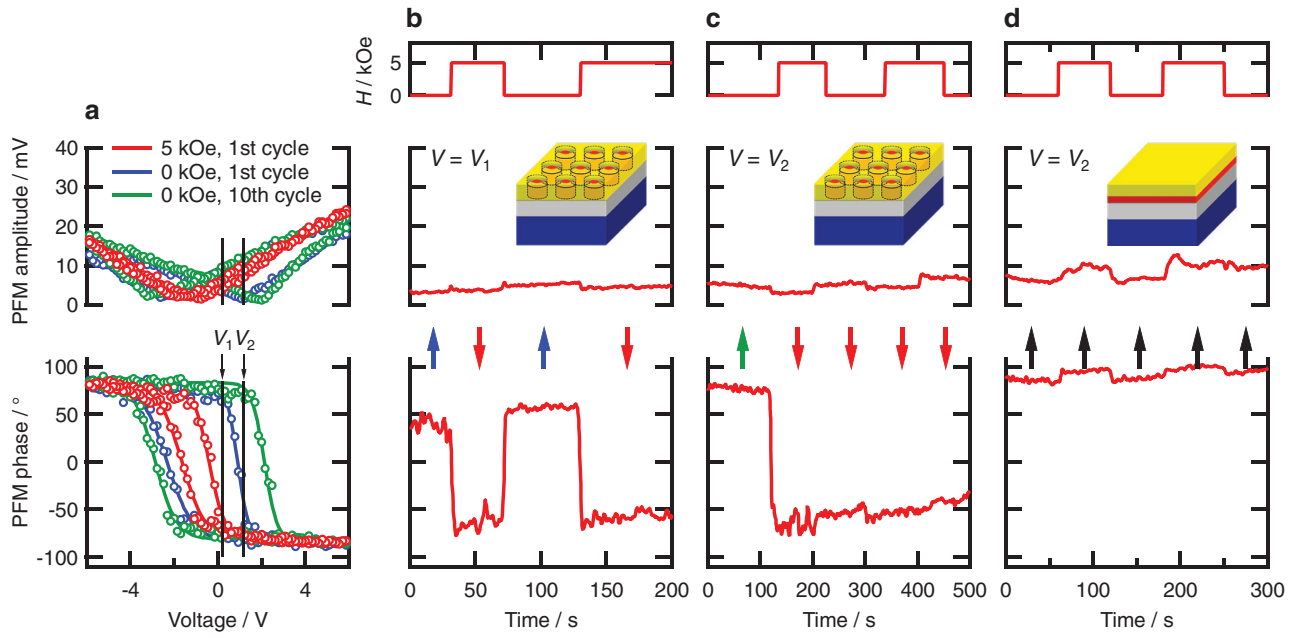

Figure 3. Switching of the electric polarization by application of a magnetic field (PFM, 300 kHz acquisition frequency). a) Ferroelectric hysteresis loops measured for the patterned sample in its nonrelaxed state at 0 (blue) and 5 kOe (red), and in its almost relaxed state at 0 Oe after ten cycles of measurement of the hysteresis loop (green); the loops are reversed compared to Figure 2a due to the change of acquisition frequency from 15 to 300 kHz. b) The nonpermanent switching of the electric polarization from the nonrelaxed 0 Oe (blue) state to the nonrelaxed 5 kOe (red) state, with the applied magnetic field shown at the top and the electric polarization shown as vertical arrows (color code as in panel (a)); the voltage applied on the sample was V_1. c) It is shown that permanent switching of the polarization is possible from the almost relaxed 0 Oe (green) state to the nonrelaxed 5 kOe (red) state; the voltage applied on the sample was V_2. d) The behavior of a bilayered control sample is shown.

Summing up, we have shown that the proper design of a nanopatterned composite layer offers the possibility to modify electrically stored information with a magnetic field, at room temperature (and most probably up to ca. 100 °C), in an intrinsically patterned medium, using a simple technology which can be reproduced in any moderately equipped laboratory. As a side benefit, although not demonstrated, the technology is compatible with flexible substrates as well, if be needed. It might be possible to achieve the same effect without having to prerelax the system, by increasing the relative deformation of the ferroelectric polymer with a proper modification of the dimensions and structure factor of the supracrystalline unit cell. Further experiments should aim at exploring the role of size, packing density, and geometry of the supracrystalline unit cell, of the interface between the two phases, and of relaxation time, and at elucidating the degree by which stresses are relaxed in the sample when repeatedly flipping the polarization by electrical or magnetic means. Replacing the conducting Ni by an insulating ferromagnetic material of even larger magnetostriction would also open extremely exciting perspectives for this new class of magnetoelectric hybrid materials, with a wealth of possible applications in data storage and sensing.[33]

Experimental Section

Materials and Preparation of the Multiferroic Layer: P(VDF-TrFE) (65 wt% of VDF units and a weight-average molar mass of ca. 300 000 g mol^{-1}) was provided by Solvay Specialty Polymers. Starting from a Si/SiO_2 substrate, a 100 nm silver (Ag) layer with 5 nm adhesive titanium (Ti) layer was deposited by thermal evaporation, followed by spincoating a ca. 75 nm P(VDF-TrFE) layer from a P(VDF-TrFE)/acetylacetone solution (35 g L^{-1}, 6500 rpm for 1 min). Then, nanoimprinting was performed on the P(VDF-TrFE) layer with an Obducat nanoimprinter (at 135 °C, 60 bar, for 10 min) using a Si mold with pillars of 65 nm diameter arranged over a square 2D lattice of 190 nm unit cell dimension; the pillar height was 90 nm. Then, Ni nanocylinders of ca. 65 nm height were grown by pulsed electrochemical deposition (–1.05 V for 10 ms and –0.7 V for 90 ms) at room temperature from an electrolyte bath containing $NiSO_4{\cdot}6H_2O$ (0.5 M) and H_3BO_3 (0.4 M) at room temperature. The potential sequence applied during the Ni electrochemical growth was controlled by a PAR 263A potentiostat using a double junction Ag/AgCl reference electrode (KCl saturated) and a platinum (Pt) counter electrode.

In the patterned control samples, Ni was replaced in the P(VDF-TrFE) matrix by Pt nanocylinders of similar height. Pt was grown by electrochemical deposition at a constant potential of –0.3 V from a commercially available "Pt-DNS" electrolyte bath (METAKEM) at 50 °C. Two other control samples were also prepared: one consisting of a spincoated ca. 80 nm thick P(VDF-TrFE) layer stacked over a continuous 25 nm thick Ni layer which was thermally evaporated on the Ag substrate; the other one having a spincoated ca. 80 nm thick P(VDF-TrFE) layer on the Ag substrate. These two samples were subsequently annealed at 135 °C for 10 min in air on a hot plate to mimic the thermal treatment of the nanoimprinted samples.

Characterization of the Multiferroic Layer: The morphology of the sample was checked by atomic force microscopy (AFM) in tapping mode and by scanning electron microscopy (SEM) in imaging mode. Magnetization curves were obtained at room temperature using an alternating gradient field magnetometer (AGFM-Lakeshore) with a maximum applied field of ±10 kOe.

The ferroelectric response of P(VDF-TrFE) was checked by PFM in contact mode (under a ca. 50 nN contact force, which was small enough

to prevent force-induced polarization switching[31]). A conductive nonmagnetic Pt/Ir coated probe was employed (SCM-PIT from Bruker, nominal spring constant 2.8 N m^{-1}, nominal tip radius 20 nm). A nonmagnetic tip holder was used; the PFM was measured by applying to the bottom electrode a small oscillating voltage of amplitude V_{ac} and frequency f_{ac}, and to the PFM tip a static voltage V_{dc}. Two working frequencies were selected, f_{ac} = 15 or 300 kHz, both far away from the contact resonance (ca. 220 kHz); the corresponding V_{ac}s were 2.5 and 2 V, respectively. When working at 15 kHz, the PFM spectroscopy curves were obtained by ramping V_{dc} from 10 to −10 V, then back to 10 V (15 V for the bilayered control sample); the ramping direction was reversed when working at 300 kHz. It was found that the width of the hysteresis loop depended on a series of parameters, such as acquisition frequency, or tip nature and bias; therefore, the measurements were always performed in strictly identical conditions to mitigate these effects. The width of the ferroelectric hysteresis loops was obtained by averaging three to four measurements performed at the same location.

The magnetic field in the vertical direction was generated by a home-made magnet equipped with a cooling system allowing to perform isothermal measurements, which was adapted into the PFM equipment below the sample. For experiments on the magnetic switching of the electric polarization with the nanopatterned P(VDF-TrFE)/Ni sample, PFM hysteresis loops were first taken at 0 or 5 kOe magnetic field (working at 300 kHz and ramping the tip bias from −10 to 10 V, then back to −10 V) in order to check the location of the switching voltage, or to relax mechanically the internal stress. The PFM phase and amplitude were then acquired ca. every 0.4 s, while the magnetic field was repeatedly switched between 0 and 5 kOe, and binomially smoothed (20 passes).

Supporting Information

Supporting Information is available from the Wiley Online Library or from the author.

Acknowledgements

The authors thank Pedro de Sá for the measurement of the magnetic properties of the samples, Florian Jurin for the growth of Pt nanowires in the control sample, and Gilles Scheen for providing guidance for Comsol modeling. Financial support was provided by the Belgian Science Policy (IAP P6/27), the Wallonia/Brussels Community (ARC 13/18-052), and the Belgian Fund for Scientific Research (FNRS).

Received: August 28, 2016
Revised: September 22, 2016
Published online: December 5, 2016

[1] T. Leydecker, M. Herder, E. Pavlica, G. Bratina, S. Hecht, E. Orgiu, P. Samori*Nat. Nanotechnol.* **2016**, *11*, 769.
[2] T. Kimura, T. Goto, H. Shintani, K. Ishizaka, T. Arima, Y. Tokura, *Nature.* **2003**, *426*, 55.
[3] N. Hur, S. Park, P. A. Sharma, J. S. Ahn, S. Guha, S. W. Cheong, *Nature* **2004**, *429*, 392.
[4] Y. Yamasaki, S. Miyasaka, Y. Kaneko, J. P. He, T. Arima, Y. Tokura, *Phys. Rev. Lett.* **2006**, *96*, 207204.
[5] D. M. Evans, A. Schilling, A. Kumar, D. Sanchez, *Nat. Commun.* **2013**, *4*, 1534.
[6] L. Keeney, T. Maity, M. Schmidt, A. Amann, N. Deepak, N. Petkov, S. Roy, M. E. Pemble, R. W. Whatmore, *J. Am. Ceram. Soc.* **2013**, *96*, 2339.
[7] W. Eerenstein, N. D. Mathur, J. F. Scott, *Nature* **2006**, *442*, 759.
[8] R. Ramesh, N. A. Spaldin, *Nat. Mater.* **2007**, *6*, 21.
[9] A. K. Tagantsev, L. E. Cross, J. Fousek, *Domains in Ferroic Crystals and Thin Films*, Springer, New York **2010**.
[10] T. Zhao, A. Scholl, F. Zavaliche, K. Lee, M. Barry, A. Doran, M. P. Cruz, Y. H. Chu, C. Ederer, N. A. Spaldin, R. R. Das, D. M. Kim, S. H. Baek, C. B. Eom, R. Ramesh, *Nat. Mater.* **2006**, *5*, 823.
[11] F. Kagawa, S. Horiuchi, M. Tokunaga, J. Fujioka, Y. Tokura, *Nat. Phys.* **2010**, *6*, 169.
[12] P. Lunkenheimer, J. Müller, S. Krohns, F. Schrettle, A. Loidl, B. Hartmann, R. Rommel, M. de Souza, C. Hotta, J. A. Schlueter, M. Lang, *Nat. Mater.* **2012**, *11*, 755.
[13] W. Qin, M. Gong, X. Chen, T. A. Shastry, R. Sakidja, G. Yuan, M. C. Hersam, M. Wuttig, S. Ren, *Adv. Mater.* **2014**, *27*, 734.
[14] W. Qin, X. Chen, H. Li, M. Gong, G. Yuan, J. C. Grossman, M. Wuttig, S. Ren, *ACS Nano* **2015**, *9*, 9373.
[15] A. Stroppa, P. Barone, P. Jain, J. M. Perez-Mato, S. Picozzi, *Adv. Mater.* **2013**, *25*, 2284.
[16] L. C. Gómez-Aguirre, B. Pato-Doldán, J. Mira, S. Castro-Garcia, M. A. Senaris-Rodriguez, M. Sanchez-Andujar, J. Singleton, V. S. Zapf, *J. Am. Chem. Soc.* **2016**, *138*, 1122.
[17] H. Zheng, J. Wang, S. E. Lofland, Z. Ma, L. Mohaddes-Ardabili, T. Zhao, L. Salamanca-Riba, S. R. Shinde, S. B. Ogale, F. Bai, D. Viehland, Y. Jia, D. G. Schlom, M. Wuttig, A. Roytburd, R. Ramesh, *Science* **2004**, *303*, 661.
[18] V. Garcia, M. Bibes, L. Bocher, S. Valencia, F. Kronast, A. Crassous, X. Moya, S. Enouz-Vedrenne, A. Gloter, D. Imhoff, C. Deranlot, N. D. Mathur, S. Fusil, K. Bouzehouane, A. Barthélémy, *Science* **2010**, *327*, 1106.
[19] C. Schmitz-Antoniak, D. Schmitz, P. Borisov, F. M. F. de Groot, S. Stienen, A. Warland, B. Krumme, R. Feyerherm, E. Dudzik, W. Kleemann, H. Wende, *Nat. Commun.* **2013**, *4*, 2051.
[20] C.-W. Nan, M. I. Bichurin, S. Dong, D. Viehland, G. Srinivasan, *J. Appl. Phys.* **2008**, *103*, 031101.
[21] A. J. Lovinger, *Science* **1983**, *220*, 1115.
[22] P. Martins, S. Lanceros-Méndez, *Adv. Funct. Mater.* **2013**, *23*, 3371.
[23] B. D. Cullity, C. D. Graham, *Introduction to Magnetic Materials*, Wiley, Hoboken **2009**.
[24] K. L. Metlov, K. Y. Guslienko, *J. Magn. Magn. Mater.* **2002**, *242–245*, 1015.
[25] S. V. Kalinin, A. Rar, S. Jesse, *IEEE Trans. Ultrason. Ferroelectr. Freq. Control* **2006**, *53*, 2226.
[26] P. Sharma, T. J. Reece, S. Ducharme, A. Gruverman, *Nano Lett.* **2011**, *11*, 1970.
[27] C.-W. Nan, G. Liu, Y. Lin, H. Chen, *Phys. Rev. Lett.* **2005**, *94*, 197203.
[28] Y. S. Oh, S. Crane, H. Zheng, Y. H. Chu, R. Ramesh, K. H. Kim, *Appl. Phys. Lett.* **2010**, *97*, 052902.
[29] Y. Wu, X. Li, A. M. Jonas, Z. Hu, *Phys. Rev. Lett.* **2015**, *115*, 267601.
[30] H. Lu, C. W. Bark, D. Esque de los Ojos, J. Alcala, C. B. Eom, G. Catalan, A. Gruverman, *Science* **2012**, *336*, 59.
[31] X. Chen, X. Tang, X. Z. Chen, Y. L. Chen, X. Guo, H.-X. Ge, Q.-D. Shen, *Appl. Phys. Lett.* **2015**, *106*, 042903.
[32] Y. Cao, Q. Li, L. Q. Chen, S. V. Kalinin, *Appl. Phys. Lett.* **2015**, *107*, 202905.
[33] J. Ma, J. Hu, Z. Li, C.-W. Nan, *Adv. Mater.* **2011**, *23*, 1062.